



Environmental toxins trigger PD-like progression via increased alpha-synuclein release from enteric neurons in mice

SUBJECT AREAS:
EXPERIMENTAL MODELS
OF DISEASE
PARKINSON'S DISEASE
DISEASES OF THE NERVOUS
SYSTEM
NEURODEGENERATION

Francisco Pan-Montojo^{1,2,5}, Mathias Schwarz¹, Clemens Winkler¹, Mike Arnhold², Gregory A. O'Sullivan⁴, Arun Pal⁴, Jonas Said¹, Giovanni Marsico⁴, Jean-Marc Verbavatz⁴, Margarita Rodrigo-Angulo⁵, Gabriele Gille², Richard H. W. Funk^{1,3*} & Heinz Reichmann^{2,3*}

Received
5 April 2012

Accepted
26 October 2012

Published
30 November 2012

Correspondence and requests for materials should be addressed to F.P.-M. (Francisco_Jose.Pan-Montojo@tu-dresden.de)

* These authors contributed equally to the work

¹Institute for Anatomy, TU-Dresden, Fetscherstr. 74, 01307, Dresden, ²Department of Neurology, University Hospital Carl-Gustav Carus, Fetscherstr. 74, 01307, Dresden, Germany, ³Center for Regenerative Therapies Dresden, Tatzberg 47/49, 01307, Dresden, Germany, ⁴Max-Planck Institute for Cell Biology and Genetics, Pfotenhauerstr. 108, 01307, Dresden, Germany, ⁵Departamento de Anatomía, Histología y Neurociencia, Facultad de Medicina, Universidad Autónoma de Madrid, Arzobispo Morcillo 4, 28029 Madrid, Spain.

Pathological studies on Parkinson's disease (PD) patients suggest that PD pathology progresses from the enteric nervous system (ENS) and the olfactory bulb into the central nervous system. We have previously shown that environmental toxins acting locally on the ENS mimic this PD-like pathology progression pattern in mice. Here, we show for the first time that the resection of the autonomic nerves stops this progression. Moreover, our results show that an environmental toxin (i.e. rotenone) promotes the release of alpha-synuclein by enteric neurons and that released enteric alpha-synuclein is up-taken by presynaptic sympathetic neurites and retrogradely transported to the soma, where it accumulates. These results strongly suggest that pesticides can initiate the progression of PD pathology and that this progression is based on the transneuronal and retrograde axonal transport of alpha-synuclein. If confirmed in patients, this study would have crucial implications in the strategies used to prevent and treat PD.

The significance of peripheral nervous system (PNS) pathology in PD has been a source of controversy over the last number of years. Different studies suggest that, in idiopathic PD (iPD) patients, PD-related pathology (Lewy Bodies and Lewy Neurites) is present in the enteric nervous system and the olfactory bulb before progressing into the central nervous system (CNS)^{1–3}. Lewy bodies (LB) and neurites (LN) are intracytoplasmatic inclusions mainly consisting of alpha-synuclein⁴. Based on these observations, Braak and colleagues developed a pathological staging of the disease that correlates well with the clinical progression of the disease^{5–7}. One hypothesis to explain Braak's staging is the ENS spreading hypothesis. It suggests that environmental insults (toxins or pathogens) acting on the PNS could trigger the appearance and progression of PD into and through the CNS.

Previously, we showed that the local effect of an environmental toxin (i.e. rotenone) on the ENS was sufficient to reproduce Braak's staging in mice⁸. Interestingly, all neuronal structures affected were primarily or secondarily connected to the ENS. Based on these results, we hypothesized that the local action of environmental toxins on the ENS leads to the appearance of PD pathology in the ENS and triggers its progression into the CNS through synaptically connected structures via the sympathetic and parasympathetic nerves.

There are different studies supporting the presence of transneuronal transport of alpha-synuclein in PD. Accumulation of alpha-synuclein was detected within grafted neurons in cerebral tissue obtained from PD patients who had received mesencephalic embryonic transplants^{9–11}. On the other hand, ex vivo and in vivo studies have shown that the alpha-synuclein observed in grafted cells came from neighboring neurons¹². Experiments using tumor-derived cell lines (e.g. neuroblastoma cells) overexpressing alpha-synuclein have shown that it can be exocytosed¹³. Altogether, these studies suggest that PD pathology progresses within the nervous system, and that, in the cases of alpha-synuclein over-expression, this progression could be based on the transneuronal transport of alpha-synuclein between different neuronal populations.



Due to the limitations of appropriate artificial promoters, current genetic models of PD using alpha-synuclein over-expression may not be able to explain the appearance and progression of the disease in most PD patients (i.e. iPD patients). Genetic forms of PD linked to alpha-synuclein account for less than 1 to 3% of typical late-onset PD and perhaps 20% of young-onset PD¹⁴ and do not show the same clinical and pathological progression pattern. Therefore, they cannot explain the appearance and progression of the disease in most PD patients. Moreover, embryonic or tumor derived cells, used as alpha-synuclein donors and acceptors, could show alterations in membrane trafficking with enhanced or reduced autophagy as observed in other cell types^{15,16}. This could have consequences in their response to external cues and internal alpha-synuclein over-expression when compared to normal neurons. All of this may lead to results that poorly reflect the true pathological conditions. Further, these results do not take into account different studies linking PD to the exposure to environmental toxins^{17,18}, especially pesticides that impair mitochondrial function, which results in increased oxidative stress¹⁹.

If our hypothesis is correct, the resection of some of the connecting nerves between the CNS and the gut (i.e. the sympathetic and parasympathetic nerves) in our mouse model should delay or block the pathological progression into the CNS and delay the appearance of motor related symptoms. On the other hand, in order to trigger the progression of PD-like pathology, pesticides must induce the abnormal secretion of a cellular component or components responsible for this progression. In this study, we tested these hypotheses using an in vivo PD model and in vitro primary cell cultures.

Indeed, our results show that the resection of sympathetic and parasympathetic nerves delays the appearance of motor symptoms and stops the progression of PD-like pathology to the previously connected neurons within the intermediolateral column of the spinal cord (IML), the vagal dorsal motor nuclei (DMV) and the substantia nigra (SN). Using enteric and sympathetic neuronal cultures, we show that rotenone induces the abnormal release of alpha-synuclein into the medium and that this alpha-synuclein can be up-taken, retrogradely transported (in neurons) and accumulated inside other cells (neuronal and non-neuronal).

Results

In order to confirm that the progression of the pathology occurred through the sympathetic and parasympathetic nerves, we performed either a hemivagotomy (i.e. the resection of the truncus vagalis anterior) or a partial sympathectomy (i.e. the removal of the nervus mesentericus inferior along the arteria mesenterica inferior) on mice prior to oral rotenone treatment. The operations had a 5% intra-operative death rate during partial sympathectomy. This was mainly caused by the accidental tearing of the arteria mesenterica inferior. The overall death rate on operated mice was of 10% in partial sympathectomized and 5% in hemivagotomized mice. We did not observe any complications or alterations in the behavior or daily life of operated mice.

Hemivagotomy and partial sympathectomy delay the appearance of motor but not gastrointestinal symptoms in oral rotenone treated mice. Throughout the treatment, we analyzed the motor and gastrointestinal functions of the mice using an accelerating protocol of the rotarod²⁰ and the 1-hour stool collection²¹ tests. In agreement with our previous study, there was a significant alteration in motor function in Non-Operated Rotenone Treated (NORT) mice when compared to CONTrols (CONT) in the third (CONT.3M: 35 ± 2.145 sec; NORT.3M: 23.711 ± 1.113 sec; $p < 0.001$) and fourth (CONT.4M: 34.211 ± 1.707 sec; NORT.4M: 21.384 ± 0.926 sec; $p < 0.001$) month of treatment as shown in Figure 1A. Remarkably, Hemivagotomized Rotenone-Treated (HRT) and Sympathectomized Rotenone-Treated (SRT) mice only showed motor alterations in the fourth (HRT.4M: 27.038 ± 1.133 , $p < 0.01$; SRT.4M:

26.038 ± 1.280 ; $p < 0.01$) but not the third month (HRT.3M: 31.75 ± 1.691 ; $p > 0.05$; SRT.3M: 32.403 ± 1.511 ; $p > 0.05$) of treatment as can be observed in Figure 1A. These results show that the appearance of motor alterations in HRT and SRT mice was delayed when compared to NORT mice.

In order to rule out the possibility of any observed difference being the effect of gastrointestinal alterations, we also analyzed whether either the hemivagotomy or the partial sympathectomy had any impact on gut motility using the 1 hour stool collection test as performed by others²¹. Animals that had survived the operation showed a decrease in gut motility in the 1-hour stool collection test one week after the operation, shown in Figure 1B. They recovered from this decrease within 3 weeks had similar gut motility values to non-operated mice by the start of treatment. This suggests that this transitory effect was due to the operation itself and not to the removal of the nerves. As shown in Figure 1C, the analysis of the intestinal function also showed that rotenone treatment decreased gut motility. NORT (NORT.1M: 0.282 ± 0.018 ; NORT.2M: 0.272 ± 0.009 ; NORT.3M: 0.245 ± 0.015 ; NORT.4M: 0.230 ± 0.009) and HRT (HRT.1M: 0.293 ± 0.013 ; HRT.2M: 0.255 ± 0.012 ; HRT.3M: 0.259 ± 0.011 ; HRT.4M: 0.228 ± 0.010) mice had a similar significant decrease in gut motility when compared to CONT (CONT.1M: 0.307 ± 0.019 ; CONT.2M: 0.340 ± 0.022 ; CONT.3M: 0.327 ± 0.018 ; CONT.4M: 0.292 ± 0.019) mice from the second month of treatment on. This suggests that the impairment in gut motility was due to the local effect of this pesticide on the ENS in both mice groups and correlates well with intestinal non-motor alterations observed in PD patients²². Interestingly, the appearance of gut motility problems was delayed in SRT mice (SRT.1M: 0.310 ± 0.027 ; SRT.2M: 0.292 ± 0.016 ; SRT.3M: 0.315 ± 0.026 ; SRT.4M: 0.225 ± 0.010), where a significant decrease in gut motility was observed only after 4 months of treatment (Figure 1C). This suggests that in these mice, despite not affecting gut motility, partial sympathectomy may have altered intestinal rotenone absorption.

Hemivagotomy and partial sympathectomy stop PD-like pathology progression into previously connected structures. We then investigated the effect of these operations in the progression of PD-related pathology (i.e. alpha-synuclein accumulation). Alpha-synuclein accumulation in the IML and the DMV nuclei was quantified on images captured from tissue sections immunostained with antibodies against of Choline Acetyltransferase (ChAT) and alpha-synuclein by using the FIJI software.

We first analyzed alpha-synuclein accumulation in the IML of CONT, NORT and SRT mice (Figure 2A–D) using a previously described image analysis method⁸. We observed a general increase of alpha-synuclein in NORT and in the upper thoracic regions of SRT mice when compared to CONT mice (Figure 2E). A detailed analysis of the different spinal cord regions showed that the amount of alpha-synuclein inside ChAT⁺ neurons of the IML was significantly increased in the thorax medium (CONT.2M: 1.221 ± 0.080 ; CONT.4M: 1.212 ± 0.032 ; NORT.2M: 1.459 ± 0.05107 ; NORT.4M: 1.460 ± 0.035), thorax inferior (CONT.2M: 1.1733 ± 0.052 ; CONT.4M: 1.209 ± 0.075 ; NORT.2M: 1.436 ± 0.072 ; NORT.4M: 1.399 ± 0.041) and thoracolumbal IML (CONT.2M: 1.114 ± 0.050 ; CONT.4M: 1.188 ± 0.049 ; NORT.2M: 1.343 ± 0.023 ; NORT.4M: 1.33 ± 0.033) of NORT mice when compared to CONT.4M mice ($p < 0.01$) after 2 and 4 months of treatment. The IML of both the thorax medium (SRT.2M: 1.195 ± 0.022 ; SRT.4M: 1.362 ± 0.022) and thorax inferior (SRT.2M: 1.223 ± 0.024 ; SRT.4M: 1.342 ± 0.024) regions (still connected to the gut of SRT mice) showed a significant increase ($p < 0.05$) in alpha-synuclein when compared to CONT.4M mice after 4 but not 2 months of treatment. This increase was comparable to 4 months treated NORT mice ($p > 0.05$). Remarkably, in SRT mice, the IML of the thoracolumbal region (corresponding to the sympathectomized ganglia) did not show an increase in

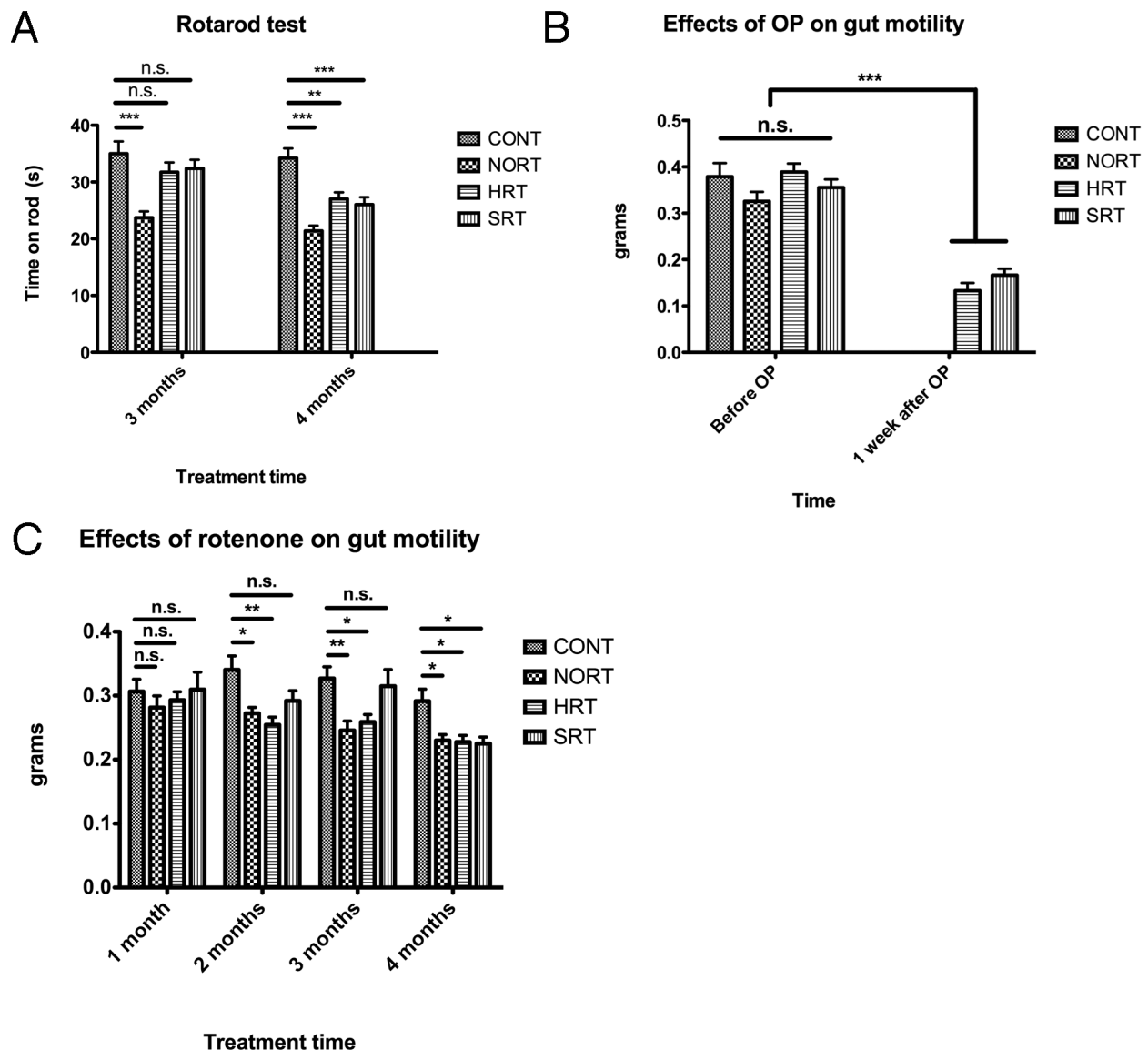


Figure 1 | Hemivagotomy and partial sympathectomy delay the appearance of motor deficits but do not induce gastrointestinal functional alterations. (A) Performance in the rotarod test using an acceleration protocol (0.3 rpm/sec) shows a delay in the appearance of symptoms in hemivagotomized or partially sympathectomized mice when compared to rotenone treated non-operated mice. (B) Bar graph showing the results of the 1-hour stool collection test one week after the operation. Hemi-vagotomized and partially sympathectomized mice show an acute transient decrease in gut motility just after the operation. (C) Bar graph showing the results of 1-hour stool test during rotenone treatment. Gut motility recovered and was equal to control until the first month of treatment. Rotenone treatment induces a progressive decrease in gut motility. CONT: control, NORT: non-operated rotenone treated, SRT: sympathectomized rotenone treated and HRT: hemivagotomized rotenone treated mice. Error bars in all graphs represent s.e.m. * is $P < 0.05$.

alpha-synuclein after 2 (SRT.2M: 1.206 ± 0.049) or 4 months (SRT.4M: 1.084 ± 0.034) when compared to CONT.4M mice ($p > 0.05$) (Figure 2E).

We then analyzed the effect of rotenone treatment on the DMV. In order to confirm that the hemivagotomy had been successful and to analyze its effect on ChAT⁺ neurons after 2 and 4 months, we estimated the number ChAT⁺ neurons in the DMV by stereological analysis using the StereoInvestigator software. It has been shown that hemi-vagotomy induces neuronal death in the DMV ipsilateral to the sectioned nerve²³. Indeed, we observed a significant reduction in the number of ChAT⁺ neurons in the DMV ipsilateral to the sectioned nerve of HRT mice when compared to the non-vagotomized DMV ($p < 0.01$). As shown in Figure 3E, this could be observed in mice examined after 2 (HRT.2M: $39.75\% \pm 6.9$) and 4 (HRT.4M: $48.86\% \pm 4.1$) months of treatment (3 and 5 months after the hemivagotomy) when compared to 4 months CONT mice (CONT.4M: 6.86%

± 4) ($p < 0.01$). Interestingly, the differences in neuronal population between 2 and 4 months HRT mice was not significant ($p > 0.05$), suggesting that the degeneration process mainly occurred during the first 3 months after the surgery.

In the brainstem, the great length of the DMV and the heterogeneity of the surrounding structures did not allow a quantitative comparison between groups as performed in the IML. Therefore, we compared the intensity of alpha-synuclein between the right and left DMV. We observed a significant increase in the amount of alpha-synuclein inside ChAT⁺ neurons of the DMV nucleus contralateral to the hemivagotomy when compared to the ChAT⁺ neurons in the ipsilateral nucleus (Figure 3C and D). This was obtained by measuring the ratio of the median fluorescence intensity (MFI) of alpha-synuclein inside ChAT⁺ neurons from the non-vagotomized side (right side, non-vagect. in Figure 3C) to the MFI of alpha-synuclein in the hemivagotomized side (left side, vagect. in Figure 3C). In all

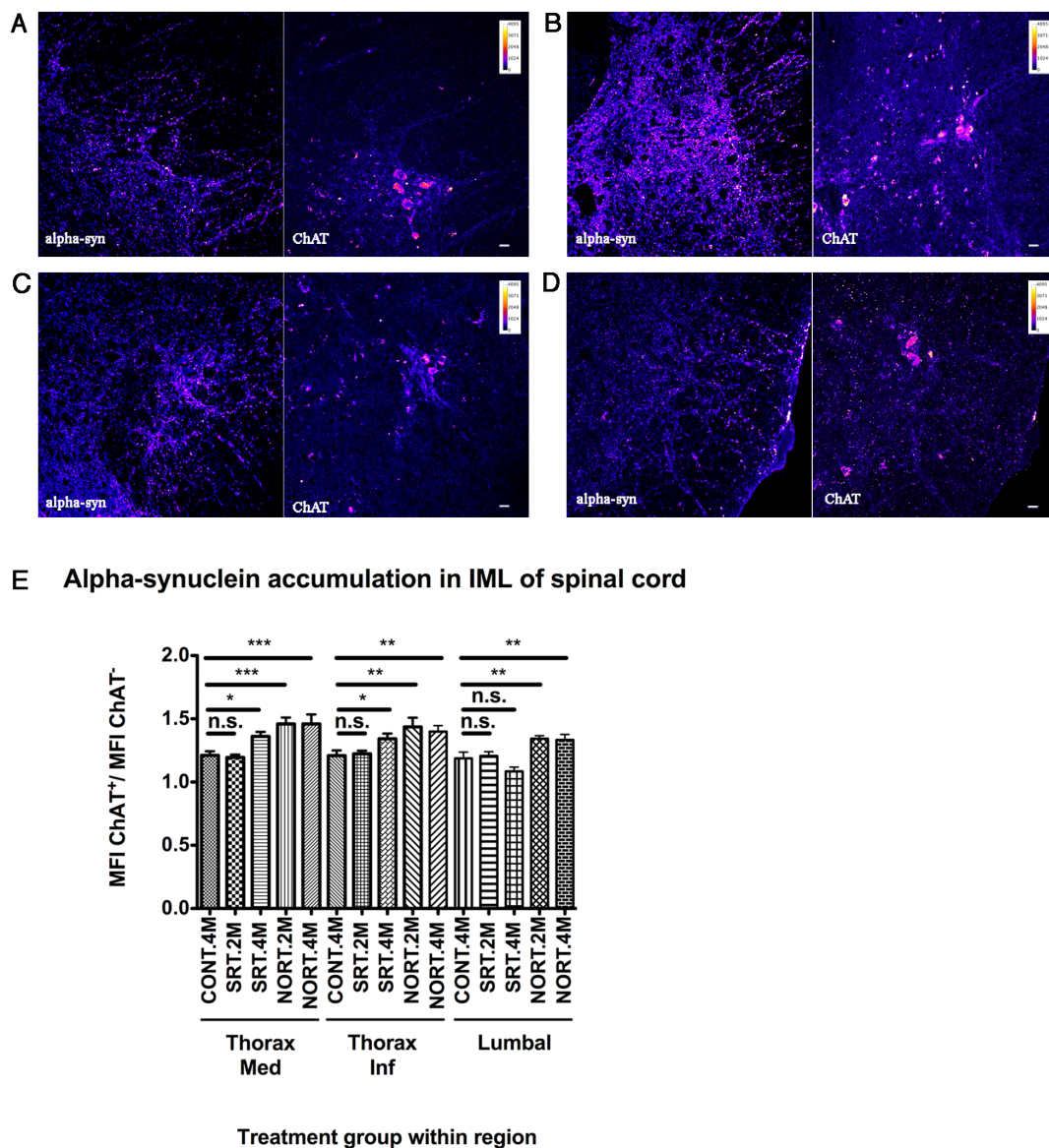


Figure 2 | Sympathectomy of the nervus mesentericus inferior inhibits alpha-synuclein accumulation in the lumbal IML nuclei. (A–D) Confocal images of thorax superior (A), thorax medium (B), thorax inferior (C) and lumbal (D) fluorescence intensity color-coded images of spinal cord sections stained with rabbit anti-alpha-synuclein or goat anti-ChAT antibodies from SRT mice 4 months after treatment. Scale bar: 20 μm . (E) Quantification of alpha-synuclein MFI rate between ChAT⁺ and ChAT⁻ areas in different regions of the spinal cord after 2 (n=8) and 4 months (n=8) of rotenone treatment. CONT: control, NORT: non-operated rotenone treated and SRT: sympathectomized rotenone treated mice. Values for CONT. 4 months (CONT.4M), NORT 4 months (NORT.4M) and SRT 2 (SRT.2M) and 4 (SRT.4M) months mice are grouped within the thoracic medium (Thorax Med.), thoracic inferior (Thorax Inf.) and the thoracolumbal (Lumbal) regions of the spinal cord. All groups for each region are compared with the CONT.4M group. Error bars represent (s.e.m.) values, n.s. is non-significant, * $P < 0.05$, ** $P < 0.005$, *** $P < 0.001$.

slides, the MFI of alpha-synuclein from both sides was normalized to the alpha-synuclein intensity in the same adjacent neutral region. This ratio was significantly increased ($p < 0.05$) in HRT mice after 4 (HRT.4M: 1.24 ± 0.048) but not 2 (HRT.2M: 1.03 ± 0.046) ($p > 0.05$) months of rotenone treatment, when compared to 2 months and 4 months NORT (NORT.2M: 0.96 ± 0.055 ; NORT.4M: 0.987 ± 0.044) and CONT (CONT.2M: 1.027 ± 0.038 ; CONT.4M: 0.971 ± 0.091) mice (Fig. 3D). Importantly, these changes occurred without further alterations in the population number of ChAT⁺ neurons inside the DMV (Figure 3E), suggesting that this increase was due to the accumulation of alpha-synuclein inside the ChAT⁺ neurons of the DMV still connected to the gut.

Hemivagotomy prevents dopaminergic cell death in the ipsilateral SN. The DMV is thought to be indirectly connected to the ipsilateral

dopaminergic neurons in the SN through multiple synapses²⁴. Therefore, we analyzed whether the hemivagotomy would have an effect on dopaminergic cell loss in the SN. For this, we compared the number of TH⁺ neurons in the SN pars compacta (SNpc) between CONT, HRT and NORT mice after 4 months of treatment (Figure 4A–C). Stereological analysis shows a significant decrease in the number of neurons in NORT mice (total TH⁺ neurons: $4,859.613 \pm 481.767$) when compared to HRT ($9,496.226 \pm 844,757$) ($p < 0.05$) or CONT ($13,032.75 \pm 188.491$) ($p < 0.01$) mice after 4 months of treatment (Figure 4D).

Finally, we also compared the amount of dopaminergic neurons in the left and right SNpc. As previously described²⁵, CONT mice had similar amount of TH⁺ neurons on both sides of the SNpc, with a left to right ratio (LRR) close to 1 (0.921 ± 0.028) (Figure 4E). Interestingly, in rotenone treated mice we observed differences in

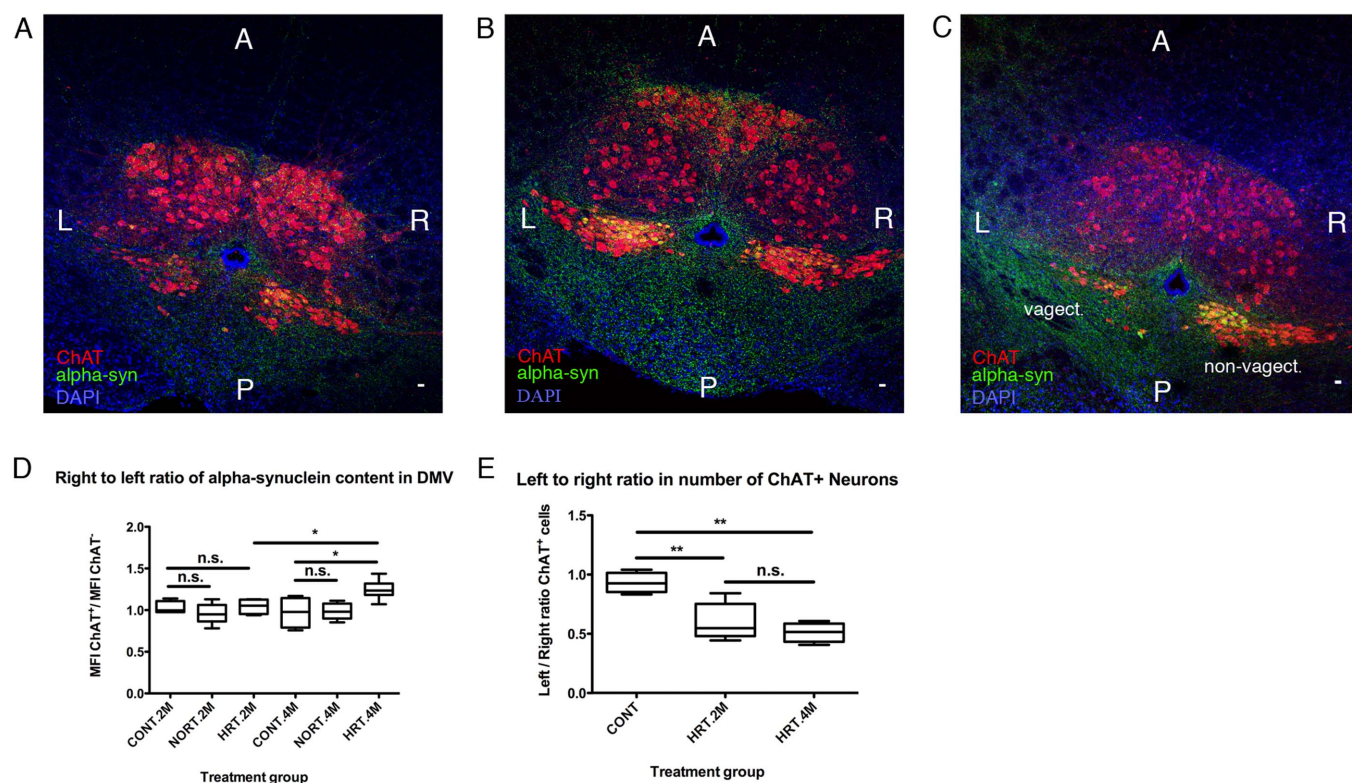


Figure 3 | Hemivagotomy prevents alpha-synuclein accumulation in the ipsilateral DMV. (A–C) Confocal images (single plane) of DMV sections stained with rabbit anti-alpha-synuclein (green) and goat anti-ChAT antibodies (red) and with DAPI (blue) obtained from (A) control (CONT) ($n=10$), (B) non-operated rotenone-treated (NORT) ($n=9$) and (C) hemivagotomized rotenone-treated (HRT) ($n=9$) mice 4 months after treatment. L, R, A and P are left, right, anterior and posterior. Scale bar: 20 μm . (D) Bar graph showing ratio between right and left alpha-synuclein MFI in the DMV of CONT, NORT, and HRT 2 (2M) and 4 (4M) months after treatment. MFI intensity values were normalized to alpha-synuclein MFI of a neutral region. (E) Bar graph showing the quantification of left to right difference in the number of ChAT⁺ neurons inside the DMV in HRT mice after 2 and 4 months compared to CONT mice after 4 months. Whiskers represent max.-min. values, n.s. is non-significant, * $P<0.05$ and ** $P<0.01$.

the lesion pattern between HRT and NORT mice. Whereas our results show a non-significant increase of the LRR in the number of TH⁺ neurons in NORT mice (1.274 ± 0.400 , $p=0.22$), we did observe a significant increase of the LRR in the number of TH⁺ neurons in HRT mice (1.982 ± 0.240) ($p<0.05$) when compared to controls (Figure 4E). This was due to a different pattern in the loss of TH⁺ neurons. In HRT mice, cell loss occurred predominantly in the right SNpc (with all left to right rate values above 1), in NORT mice the laterality of the lesion changed from animal to animal with rate values both above and under 1. Moreover, the number of TH⁺ neurons in the SNpc ipsilateral to the hemivagotomy (i.e. the left side) in HRT mice ($6,217.483 \pm 254.993$) did not differ ($p \gg 0.05$) from the number of dopaminergic cells in the left side of the SNpc in CONT mice ($6,244.027 \pm 102.864$) (Figure 4F). Thus, suggesting that the hemivagotomy prevented cell death in the ipsilateral SNc.

Taken together, these results show that the resection of some of the nerves connecting the CNS to the ENS is sufficient to prevent the progression of the pathology to the previously connected structures, delay the appearance of motor symptoms and prevent cell death in the ipsilateral SN. Intriguingly, the amount of alpha-synuclein inside the IML of both thorax medium and inferior regions in SRT.2M mice was comparable to that of CONT.4M mice and significantly lower than that of NORT.2M littermates, suggesting an effect on rotenone absorption after this operation (see Discussion).

Rotenone induces alpha-synuclein release in enteric and sympathetic neurons. In order to further investigate the underlying molecular mechanism of PD pathology progression, we used primary neuronal cell cultures. Results from recent studies done ex

vivo¹³, in animal models¹² and in autopsy material from PD patients¹¹, suggest that the transneuronal transport of alpha-synuclein could play a role in PD progression. Therefore, we analyzed the effect of rotenone on alpha-synuclein secretion using sympathetic and enteric primary neuronal cultures. In enteric neuronal cell cultures, the number alpha-synuclein inclusions inside non-neuronal cells was increased (Control: 0.215 ± 0.051 ; 10 nM: 0.417 ± 0.115 (n.s.); 50 nM: 0.683 ± 0.251 ($p<0.05$); 100 nM: 1.039 ± 0.3358 ($p<0.01$)) upon rotenone treatment (Figure 5A–E). We then treated non-neuronal intestinal cells with rotenone in the absence of neurons to exclude the possibility of endogenous alpha-synuclein expression being affected by rotenone treatment. We did not observe any alpha-synuclein inside these cells under these conditions (data not shown). This agrees with previous studies showing that levels of alpha-synuclein in non-neuronal cells are minor compared to that found in neurons²⁶ and suggests that environmental toxins like pesticides can trigger the transfer of alpha-synuclein from enteric neurons to neighboring non-neuronal cells.

If alpha-synuclein is released from enteric neurons into the medium, then extracellular alpha-synuclein should be detectable. Indeed, free-floating mCherry-alpha-synuclein could be detected by live cell imaging of enteric neurons expressing mCherry-alpha-synuclein (Movie 1). To confirm that alpha-synuclein in culture was increased by the presence of rotenone in neurons without the artificial over-expression of alpha-synuclein, we sought to determine the extracellular presence of alpha-synuclein. Our mixed enteric neuron cultures were deemed unsuitable, since the majority of the released alpha-synuclein was assumed to be taken up by the neighboring non-neuronal cells, as shown by our immunofluorescent data (Figure 5A–E).

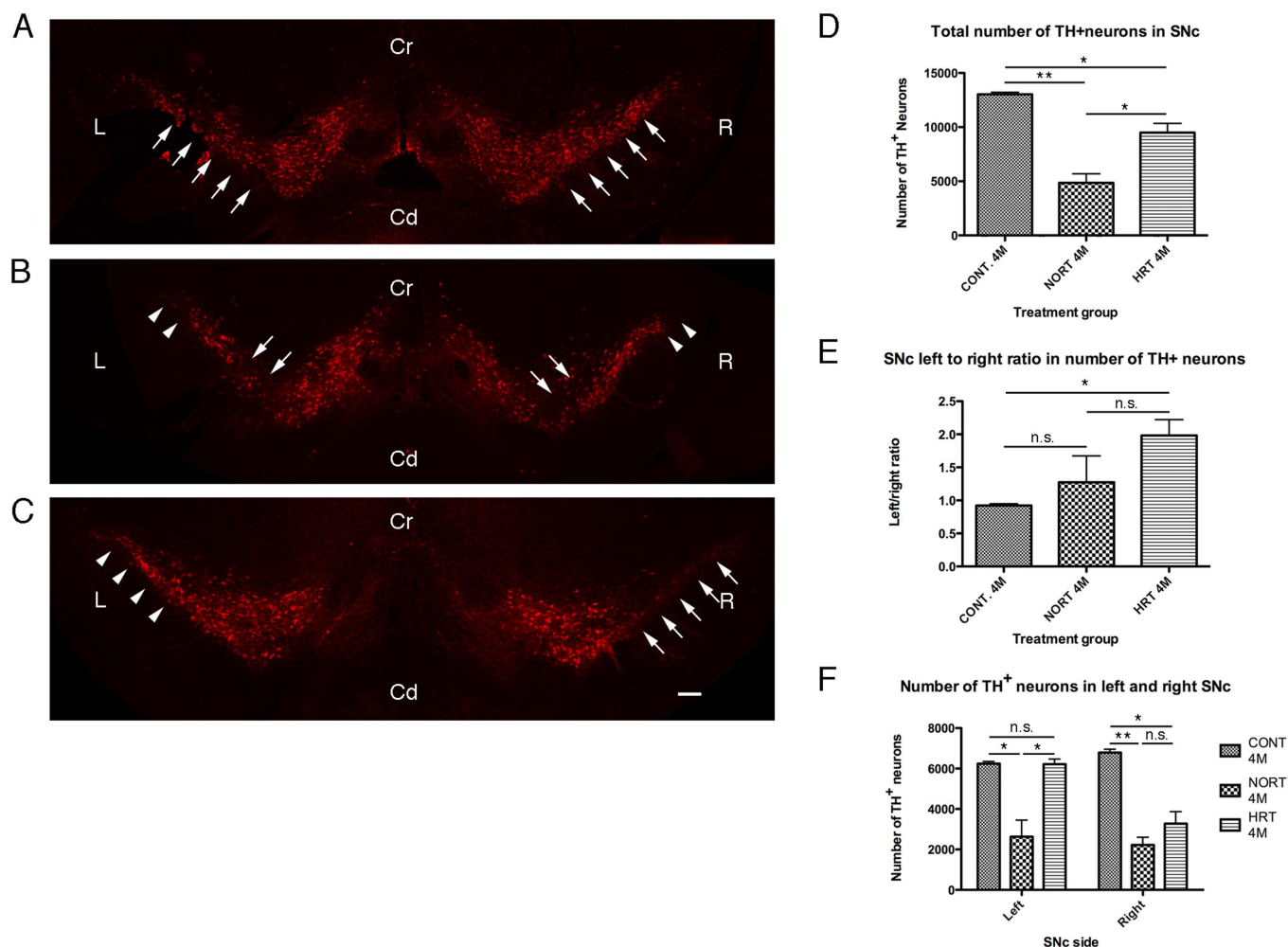


Figure 4 | Hemivagotomy prevents dopaminergic cell death in the ipsilateral SNc. (A–C) Stitched fluorescence microscope images of 40 μm brain mesencephalic sections from 4 months CONT. 4M: control (A), NORT. 4M: non-operated rotenone treated (B) and HRT. 4M: hemivagotomized rotenone treated (C) mice. Brain sections were stained with sheep anti-tyrosine hydroxylase (TH) antibody (red). L, R, Cr and Cd are left, right, cranial and caudal. Scale bar represents 200 μm . TH⁺ neurons density in the SNc is diminished in NORT mice (B) when compared to CONT (A) and HRT (C) mice. In NORT mice, a clear reduction can be observed in the lateral (arrowheads in B) and medial (arrows in B) SNc when compared to CONT mice (arrows in A). A reduction in the density of TH⁺ neurons can be observed in the lateral part of the right SNc (arrows in (C)) when compared to the contralateral SNc (arrowheads in (C)). (D–F) Bar graphs showing the quantification of the total number of TH⁺ neurons in the SNc (D), the left to right ratio in the number of TH⁺ neurons within the SNc (E) and the amount of neurons in the left or right SNc (F) in CONT, NORT and HRT mice. Error bars represent (s.e.m.), n.s. (non-significant), * $P < 0.05$, ** $P < 0.01$.

Interestingly, the amount of alpha-synuclein inside non-neuronal cells was directly proportional to the concentration of rotenone. As expected, we were unable to detect any alpha-synuclein in the $10,000 \times g$ or $100,000 \times g$ fraction (exosomal fraction) of the medium collected from control or rotenone treated neurons (data not shown). Therefore, we performed the same experiment on untreated, control (vehicle treated), 0.1 μM , 1 μM and 5 μM rotenone treated sympathetic neurons. These neurons can be isolated and cultured with a higher degree of purity and the growth of contaminating non-neuronal cells is inhibited by the presence of 1 μM cytosine arabinoside. Indeed, alpha-synuclein was detected in the exosomal fraction of the medium obtained from the sympathetic neuronal cultures treated with rotenone but not from the untreated or control cultures (Exo. in Figure 6A). Intriguingly, we also observed even higher amounts of alpha-synuclein in the pellet from the $10,000 \times g$ centrifugation in these same treatment groups (Non-exo. in Figure 6A). This pellet was expected to contain little or no exosomes. In order to determine whether the alpha-synuclein observed in this fraction was due to the presence of exosomes, we analyzed both fractions from two different conditions (vehicle and

0.1 μM rotenone) using a negative staining in electron microscopy. As expected, we could observe that the majority of the structures in the exosomal fraction resembled exosomes (Figure 6B–C) and only a few exosomal-like structures were observed in the $10,000 \times g$ fraction (Figure 6B–C). In both cases, these membrane structures had the characteristic size distribution of exosomes with the majority of particles having a diameter between 80 and 100 nm (Figure 6B). Finally, we analyzed the number of exosomes per condition in the $10,000$ and $100,000 \times g$ fractions. The number of exosomes was significantly increased after rotenone treatment in both fractions (Figure 6D). These results suggest that rotenone treatment increases exocytosis and alpha-synuclein release. It also supports data from two previous opposite but complementary studies^{13,27}, one suggesting that the release of alpha-synuclein into the extracellular medium occurs through exocytosis inside exosomes and the other claiming that it occurs outside them. In order to test both hypotheses, we performed an immunogold staining against alpha-synuclein. We observed gold particles outside and inside exosomal structures, attached to lipid membranes or on fibrillar extracellular structures in both conditions (Figure 6E–G). Thus, confirming the presence of

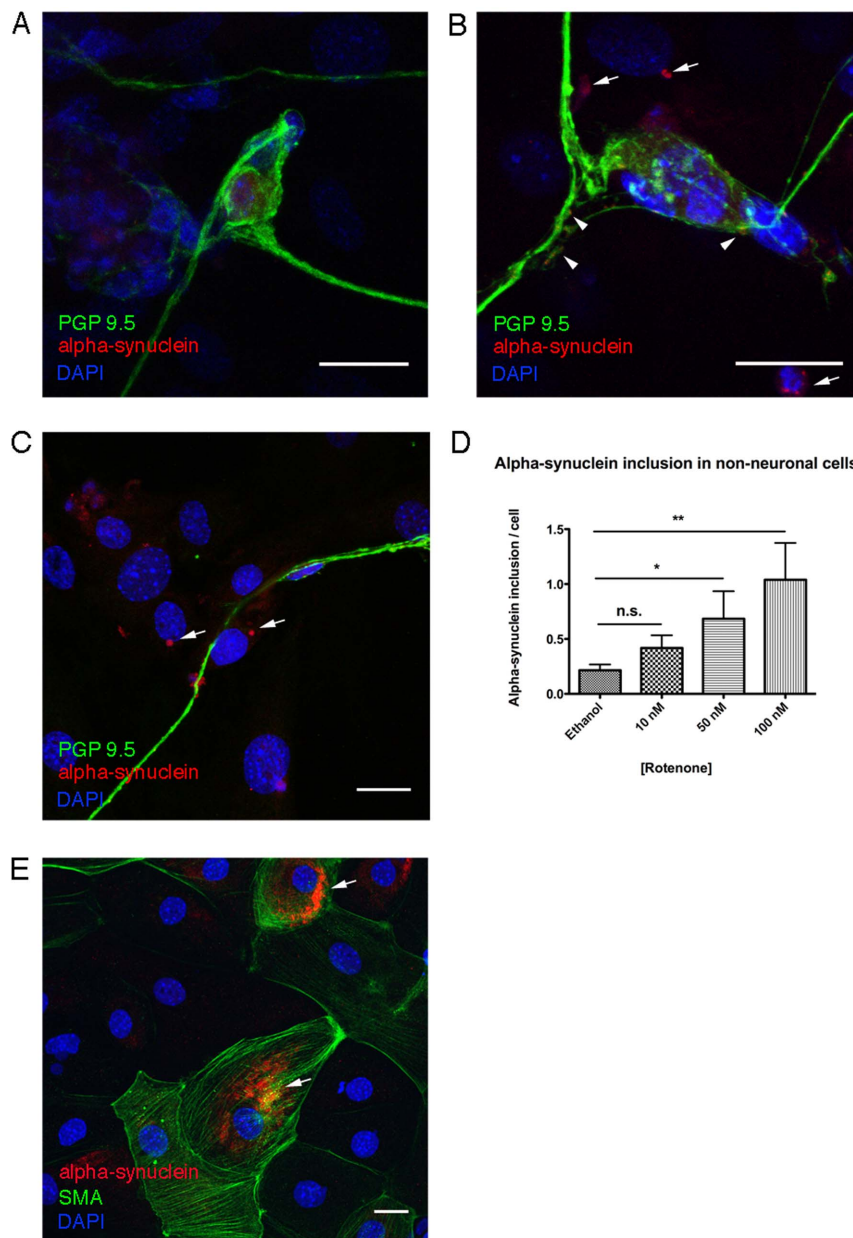


Figure 5 | Rotenone induces alpha-synuclein release in sympathetic and enteric primary neuronal cultures. (A–C) Confocal images (maximum projection) of enteric cell culture expressing endogenous alpha-synuclein after control (A) or rotenone ((B) and (C)) treatment and subsequently stained with rabbit anti-protein related peptide 9.5 (PGP 9.5) (green) and mouse anti-alpha-synuclein (red) antibodies and DAPI (blue). All scale bars in this figure represent 20 μm . Alpha-synuclein inclusions in non-neuronal cells can be observed only after rotenone treatment (arrows in (B) and (C)). They are usually localized around the nucleus inside non-neuronal cells surrounding enteric somas (B) and neurites (C). Rotenone treatment also increases enteric intraneuronal alpha-synuclein (arrowheads in (B)). (D) Bar graph showing quantification of alpha-synuclein inclusions per non-neuronal cells after Ethanol (Vehicle), 10, 50 and 100 nM rotenone treatment. Error bars represent (s.e.m.), n.s. (non-significant), * $P < 0.05$, ** $P < 0.01$. (E) Confocal images (maximum projection) of enteric cells stained with rabbit anti-Smooth Muscle Actin (SMA, green) and mouse anti-alpha-synuclein (red). Alpha-synuclein can be observed inside SMA⁺ cells (arrows in (E)).

alpha-synuclein and suggesting that it is released outside and inside these structures.

Secreted alpha-synuclein is actively up-taken by axon terminals and retrogradely transported to the soma of sympathetic presynaptic neurons, where it accumulates. Finally, we wanted to investigate whether released alpha-synuclein could also be taken up via synaptically connected structures like the sympathetic ganglionic neurons. First, we co-cultured sympathetic neurons on top of enteric neurons expressing mCherry-alpha-synuclein. Within days, mCherry-alpha-synuclein could be observed accumulating

inside tyrosin hydroxylase (TH)⁺ sympathetic neurons (Figure 7A). However, this system does not completely mimic the sympathetic innervation of the ENS in vivo and does not differentiate between somal and axonal up-take of alpha-synuclein. In vivo, sympathetic neuronal somas are located within the sympathetic ganglia whereas the synaptic connection with the enteric neurons occurs much further at the gastrointestinal wall. Therefore, sympathetic somas and neurites are located in two different unrelated extracellular environments.

In order to better mimic the physiological sympathetic innervation of the gut, we combined for the first time two different methods:

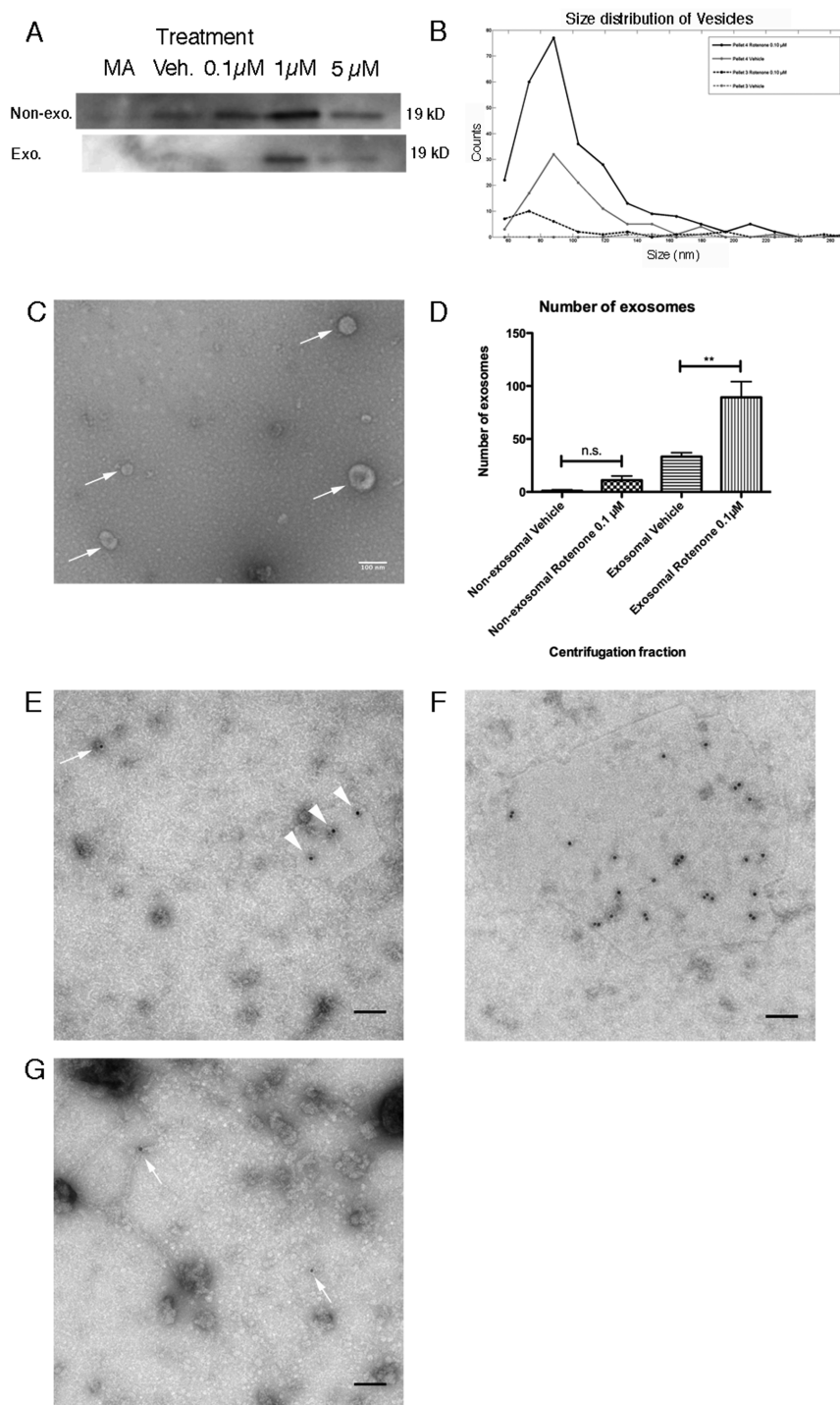


Figure 6 | Alpha-synuclein is secreted inside and outside exosomes upon rotenone treatment. (A) Western-blot of $10,000 \times g$ (non-exosomal) and $100,000 \times g$ (exosomal) fraction isolated from the medium collected from control (MA), vehicle (Veh), 0.1 μM , 1 μM and 5 μM rotenone treated primary sympathetic neuronal cultures. Blots were probed with a rabbit anti-alpha-synuclein antibody. (B) Size distribution of exosomal structures in exosomal (Pellet 4) and non-exosomal (Pellet 3) centrifugation fractions treated with rotenone (Rotenone 0.1 μM) and vehicle (Vehicle). (C) Electron microscopy images of the exosomal fraction. Scale bar: 100 nm. Arrows in (C) show exosome-like structures. (D) Graph showing the number of exosomes per field in control (vehicle) and treated (Rotenone 0.1 μM) samples corresponding to the exosomal and non-exosomal fractions. Error bars represent (s.e.m.), n.s. (non-significant), $**P < 0.01$. (E-G) Electron microscopy images of the exosomal (E-F) and non-exosomal (G) fractions labeled with gold against alpha-synuclein. Immunogold labeling can be observed on exosomal structures (arrow in (E)) and on lipid membranes (arrowheads in (E)). Alpha-synuclein seems to be enhanced on lipid membranes (black circles in (F)) and gold particles can also be observed on extracellular fibrillar structures in the non-exosomal fraction (arrows in (G)).

Campanot chambers and glass beads coated with PLL. Campanot chambers allow the compartmented culture of sympathetic neurons and have been previously used to analyze the effect of molecular

signals on neurite growth^{28,29}. In this system, sympathetic somas are plated in one compartment of the chamber and their neurites grow underneath a divider to the next compartment (Figure 7B).



Adjacent compartments are leak-proof, so that culture mediums do not mix.

We then introduced a new component to this system: enteric neurons cultured on top of PLL-coated glass beads. Enteric neurons can be easily cultured on top of PLL-coated glass beads, where they quickly spread their neurites over several beads (Figure S1A and B in Supplementary Data). One of the main advantages of culturing neurons attached to glass beads is that mature neurons can be easily manipulated and transferred between wells by simply moving the beads³⁰. Remarkably, we could observe synaptic-like connections

between sympathetic and enteric neurons when these were placed on top of sympathetic neurons (Figure S1D in Supplementary Data). For our experiments, we infected enteric neurons with a lentivirus carrying mCherry-alpha-synuclein (see Figure S1C Supplementary Data) and removed all lentiviruses from the medium through several medium changes before transferring them to the Campenot chamber. After sympathetic neurites had grown into the next compartment, we added cherry-alpha-synuclein expressing enteric neurons to this compartment and cultured them together for one week (see Figure 7B). Because enteric neurites are not strong

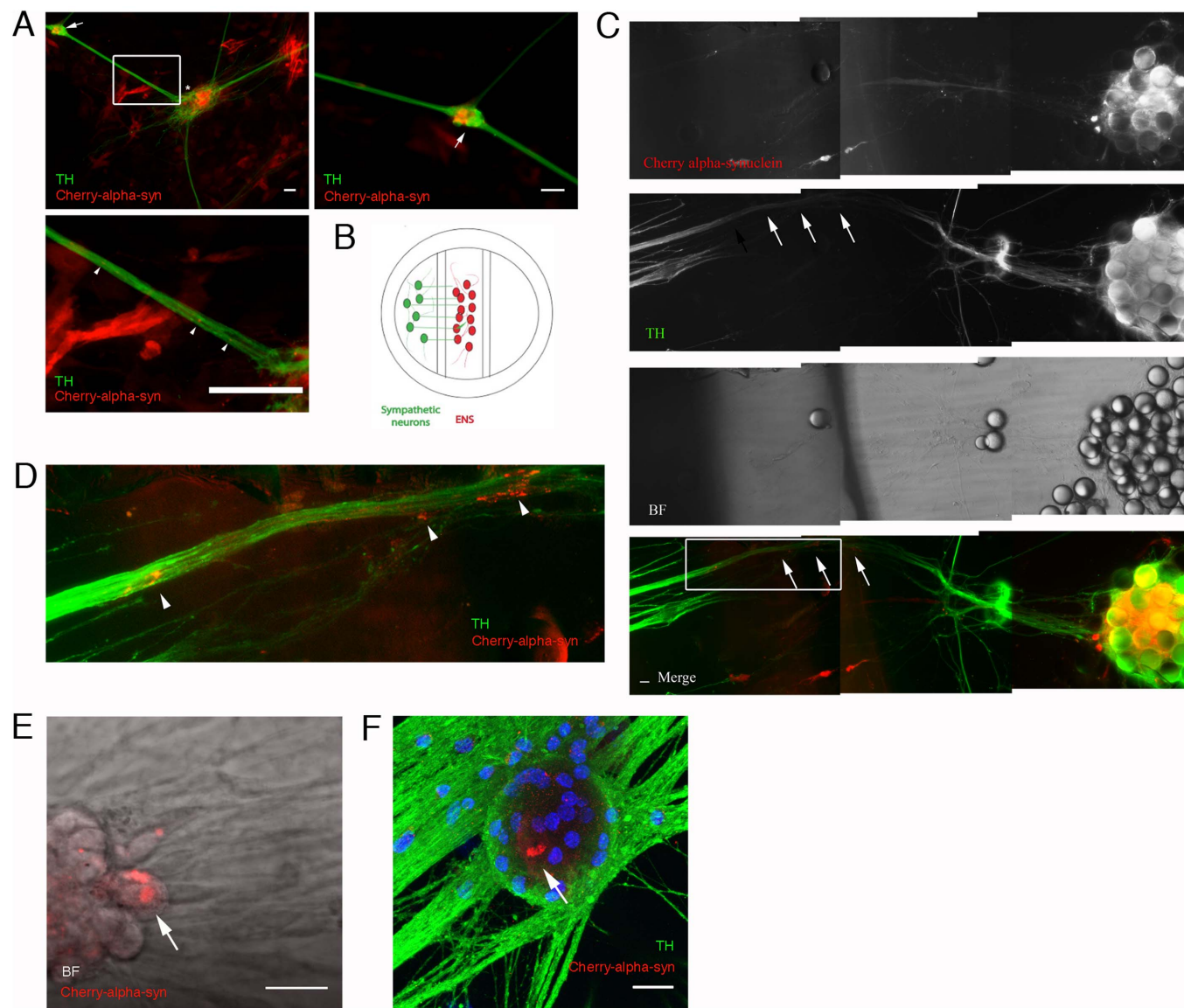


Figure 7 | Released enteric alpha-synuclein can be up-taken and retrogradely transported by sympathetic neurons. Scale bars are 20 μm in all images. (A) Fluorescence microscope images of co-cultured ENS cells expressing mCherry-alpha-synuclein (red) and sympathetic neurons stained with a rabbit anti-TH antibody (green) ($n=3$). Sympathetic neurons (arrows in the upper left image in A are in contact with mCherry-alpha-synuclein enteric neurons (*). Upper right image in panel A shows another image of the sympathetic neuron marked with an arrow in the upper left image highlighting the somal accumulation of mCherry-alpha-synuclein (arrow). Lower left image in panel A shows a zoomed in region of TH+ neurites in contact with mCherry-alpha-synuclein expressing enteric neurons framed in the upper left image. mCherry-alpha-synuclein can be observed inside sympathetic neurites (arrowheads). (B) Schematics of the Campenot chamber with sympathetic neurons in green and enteric neurons in red. (C) Montages of microscopy low magnification images from Campenot chambers corresponding to the region underneath the divider and the proximal neurite compartment. Sympathetic neurons were stained with rabbit anti-TH antibody (green) and enteric neurons express cherry-alpha-synuclein (red). Each row of images represents different channels (from top to bottom: cherry-alpha-synuclein, TH, bright-field (BF)) and a merge. Sympathetic TH+ neurons can be observed under the divider and forming a dense network around cherry-alpha-synuclein expressing enteric neurons. (D) Zoomed in region of the sympathetic neurites framed in (C). Cherry-alpha-synuclein can be observed along sympathetic neurites under the divider. (E) Confocal images showing cherry-alpha-synuclein (red) accumulating inside sympathetic TH+ neurons in grey (BF) and green in F.



enough to cross the divider, this system can also mimic the unidirectionality of the sympathetic innervation on the gut.

Using bright-field microscopy we could observe a profuse sympathetic neurite network covering the glass beads already after a few days. This observation was confirmed by immunostaining against TH (Figure 7C). Interestingly, we also observed cherry-alpha-synuclein inclusions inside sympathetic neurites and soma underneath the divider (Figures 7C and D) and in the sympathetic compartment of the chamber (Figures 7E and F). This suggests that alpha-synuclein had been up-taken by sympathetic neurites and retrogradely transported into the soma. We confirmed this by using live-cell imaging, where cherry-alpha-synuclein particles could be observed moving along sympathetic neurites (Video 2 in Supplementary Data).

Discussion

The significance of PNS pathology in PD pathophysiology and clinical non-motor symptoms has been a source of controversy over the last number of years. Many authors believe that the localization of these lesions could be explained by neuronal type specific sensitivity against a global insult to the nervous system^{31–33}. However, more recent studies suggest that there is a progression of the disease across the nervous system and that environmental factors are strongly associated with the appearance of PD^{31,11}.

The results of our study support the latter hypothesis by showing that: i) PD-like pathology progression *in vivo* depends on cell-to-cell transmission between neurons of the peripheral and central nervous system, ii) dopaminergic cell death in the SNc relies on an intact multi-synaptic path, iii) the application of an environmental toxin (rotenone) on enteric neurons is sufficient to induce PD-like pathology and to trigger the release of alpha-synuclein from the enteric neurons into the extracellular matrix, iv) alpha-synuclein released by enteric neurons exposed to rotenone can be taken up either by non-neuronal cells or presynaptic neurons and v) released enteric alpha-synuclein can be up-taken at the presynaptic neurites and retrogradely transported to the soma, where it accumulates.

Intriguingly, in both groups that underwent an operation (i.e. HRT and SRT) differences in the amount of alpha-synuclein within ChAT⁺ neurons inside IML and DMV regions still connected to the gut could only be observed after 4 months of treatment. NORT mice, on the other hand, had increased alpha-synuclein levels in these same regions already after 2 months. This correlates well with the data from our previous study⁸ and suggests a delay in the increase of alpha-synuclein in SRT mice.

In HRT mice, this apparent delay could be explained by a transient increase in intracellular alpha-synuclein inclusions. This has been previously observed in neurons undergoing retrograde axonal degradation after an axotomy³⁴. As we measured alpha-synuclein accumulation specifically inside ChAT⁺ neurons and there was no cell death between the 2 and 4 month of treatment, it can be assumed that right to left differences in alpha-synuclein after 4 months are due to changes in alpha-synuclein content in the right DMV rather than cell death or variations in extracellular alpha-synuclein. It also suggests that this effect was due to the interruption of the gut-DMV axis and not to any substance present systemically (i.e. rotenone or its derivatives). A systemic effect would affect ChAT⁺ cells in both sides. In this case, we would not have observed any right to left differences in alpha-synuclein content inside ChAT⁺ neurons. A priori, this explanation could only be applicable to HRT mice. In SRT mice, only ganglionic sympathetic neurites were sectioned during the surgery. Therefore, IML neurons did not suffer a direct axotomy in SRT mice. However, it cannot be excluded that the degradation of ganglionic sympathetic neurons had an effect on ChAT⁺ neurons of the IML.

Another possible explanation for the delay observed in SRT mice is that, while not affecting gut motility, partial sympathectomy leads to

a decreased intestinal absorption of rotenone. Different studies have shown that chemical sympathectomy leads to hyperproliferation of the intestinal mucosa increasing the thickness of the wall^{35,36}. On the other hand, increased adrenergic activity enhances the permeability of the intestinal wall^{37,38}, so it can be assumed that the lack of sympathetic innervations decreases it. Both situations would explain an impaired rotenone absorption in SRT mice resulting in decreased rotenone concentrations acting on the ENS. This could delay the appearance and progression of the pathology to still connected structures. Nevertheless, the low levels of alpha-synuclein in the lumbal IML of SRT mice compared to those of NORT mice even after 4 month of treatment are comparable to the ones observed in CONT mice. This can only be due to the effect of the sympathectomy itself, confirming our hypothesis.

Remarkably, hemivagotomy seems to protect against dopaminergic cell death in the SNc ipsilateral to the hemivagotomy. As previously described²⁵, the number of dopaminergic neurons between the right and left SN did not significantly differ in CONT mice, with a left to right ratio around 1. In this study, we observed dopaminergic cell death and laterality of the neuronal lesion in both NORT and HRT mice after oral rotenone treatment. However, cell death in HRT mice is significantly decreased when compared to NORT mice. This nicely correlates with the results observed in the rotarod test. Interestingly, whereas in NORT mice neuronal death can be increased in the left or right SN depending on the animal, hemivagotomized mice show a higher consistency in the laterality of the lesion with around 50% less dopaminergic neurons in the SNc contralateral to the hemivagotomy and a normal amount of dopaminergic neurons in the SNc ipsilateral to the hemivagotomy. The amount of TH⁺ neurons in the SNc that we observe in CONT and in the ipsilateral SNc in HRT mice coincide with that observed by others using the same stereological method²⁵. Such strong differences between left and right SNc, as the ones observed in HRT mice, have only been described using unilateral striatal injections of 6-OHDA³⁹, where there is up to a 90% reduction in the number of dopaminergic neurons inside the SN of the injured side. To our knowledge, no other animal model of PD, even those using systemic administration of toxins, show such laterality in the damage of the SN. Finally, we also observed a bigger loss of dopaminergic neurons when compared to our previous results in 3 months rotenone-treated mice. These results strongly support our hypothesis showing that, indeed, PD-like pathology progression can reach the SN through vagus nerve upstream connected structures.

Altogether, these results strongly suggest that PD-like pathology progression occurs through sympathetic and parasympathetic nerves and that the scission of these nerves is sufficient to stop the progression of the pathology into the CNS.

Further studies on the pathophysiological relevance and the precise molecular mechanisms underlying the neuron-to-neuron transmission of alpha-synuclein are still needed. It is not clear whether alpha-synuclein is released inside or outside exosomes. The relative low amounts of exosomes in comparison to the amounts of alpha-synuclein in the 10.000 × g fraction, suggests that the majority of alpha-synuclein was not on or in exosomes in our samples. Regrettably, the data from the EM-immunogold staining does not help to clarify this. EM-Immunogold shows alpha-synuclein inside and outside exosomes. Interestingly, big amounts of alpha-synuclein also appear bound to lipidic membranes. The reason for this last observation remains unclear. Finally, it cannot be excluded that the alpha-synuclein released from the neurons inside exosomes is freed as a result of sample handling (i.e. freezing), allowing the release of alpha-synuclein into the medium. Other questions that remain unanswered are related to the molecular mechanisms and players implicated in the endocytosis/retrograde axonal transport of alpha-synuclein and the effect of endocytosed alpha-synuclein on the presynaptic neuron.



Our *in vitro* results and that from others^{9,12,13,40} suggest that trans-neuronal transport of alpha-synuclein could be the underlying mechanism responsible for the pathology progression in iPD patients. In support of this hypothesis, it has been shown that alpha-synuclein is sufficient for the induction of pore formation, mitochondrial dysfunction and oxidative stress through the alteration of microtubule dynamics^{41–44}. Other study showed that endocytosed alpha-synuclein is present inside Lewy body-like inclusions in acceptor cells¹². Finally, a recent study has shown that alpha-synuclein is transported between cells in its aggregated form⁴⁰. Interestingly, they also have shown that alpha-synuclein is present outside and inside exosomes. Combined, these results indicate that endocytosed-aggregated alpha-synuclein could perpetuate and maintain the pathology on the presynaptic neuron through at least two non-exclusive mechanisms: i) alpha-synuclein can act either as a nucleation factor allowing its own recruitment to form alpha-synuclein aggregates and/or ii) it can extend the effect of rotenone through the inhibition of the mitochondrial complex I on the presynaptic neuron. This latter hypothesis seems more plausible, as it would also explain other pathological alterations observed in PD patients like the presence of radical oxygen species or the inhibition of mitochondrial Complex I inside affected neurons. Finally, it has been shown that different neuronal types have different sensitivities to Complex I inhibition-mediated toxicity, suggesting the presence of dopamine-containing vesicles as responsible for enhanced toxicity in dopaminergic neurons⁴⁵.

All these different aspects of the same process involving alpha-synuclein transport could explain both the pathological and clinical staging of PD. Differences in the severity between motor and non-motor clinical symptoms of PD can be due to the neuronal-type specific sensitivity to alpha-synuclein-induced oxidative stress.

We believe that the newly developed *in vitro* model mimicking the sympathetic innervation of the ENS will be a very valuable tool to answer these questions and perform drug screenings. It can be easily manipulated and has got clear read out parameters (e.g. the dynamics of cherry-alpha-synuclein transport inside sympathetic neurites or the presence or absence of alpha-synuclein inside sympathetic soma). Overall, our results potentially have important implications in the diagnosis and treatment of PD, as they support the ENS-spreading hypothesis and suggest new early diagnosis screening and pharmacological targets to tackle this disease.

Methods

All animal experiments were carried out in accordance with the National Institutes of Health Guide for the Care and Use of Laboratory Animals, that had been approved by the Saxonian Committee for Animal Research, Dresden, Germany, EU. Materials and methods are described in the supplementary data. Briefly, for the *in vivo* experiments, mice were divided in 8 groups ($n=10$) with 4 different treatments (control, rotenone treated, rotenone treated after hemivagotomy and rotenone treated after partial sympathectomy) and two treatment times (2 and 4 months). Motor and gastrointestinal functions were analyzed once a month with the help of the rotarod and 1-hour stool collection tests during treatment. After treatment, animals were sacrificed and perfused with 4% PFA for immunohistological staining and image analysis.

In vitro experiments were performed on primary neuronal cell cultures using enteric or sympathetic neurons isolated from postnatal mice (P1–P5). Exosome isolation was performed on equal amounts of media from the same treatment day that were collected and pooled together as previously described⁴⁶. For some experiments, enteric neurons were transfected with a lentivirus carrying mCherry-alpha-synuclein.

Statistical analysis. Data comparisons were made with anova and non-paired or paired *t*-tests as appropriate using GraphPad Prism® (GraphPad Software, Inc., La Jolla, CA, USA), significance being $p \leq 0.05$, whiskers representing max.-min. and bars representing the standard error of the mean (s.e.m.). For every group statistics are represented as follows: Group name: mean \pm s.e.m.

1. Wakabayashi, K., Takahashi, H., Ohama, E. & Ikuta, F. Parkinson's disease: an immunohistochemical study of Lewy body-containing neurons in the enteric nervous system. *Acta Neuropathol* **79**, 581–583 (1990).
2. Braak, H., de Vos, R. A., Bohl, J. & Del Tredici, K. Gastric alpha-synuclein immunoreactive inclusions in Meissner's and Auerbach's plexuses in cases staged for Parkinson's disease-related brain pathology. *Neurosci Lett* **396**, 67–72 (2006).

3. Braak, H., Sastre, M., Bohl, J. R., de Vos, R. A. & Del Tredici, K. Parkinson's disease: lesions in dorsal horn layer I, involvement of parasympathetic and sympathetic pre- and postganglionic neurons. *Acta Neuropathol* **113**, 421–429 (2007).
4. Spillantini, M. G. *et al.* Alpha-synuclein in Lewy bodies. *Nature* **388**, 839–840 (1997).
5. Braak, H., Ghebremedhin, E., Rub, U., Bratzke, H. & Del Tredici, K. Stages in the development of Parkinson's disease-related pathology. *Cell Tissue Res* **318**, 121–134 (2004).
6. Wolters, E. & Braak, H. Parkinson's disease: premotor clinico-pathological correlations. *J Neural Transm Suppl* 309–319 (2006).
7. Hawkes, C. H., Del Tredici, K. & Braak, H. A timeline for Parkinson's disease. *Parkinsonism Relat Disord* **16**, 79–84.
8. Pan-Montojo, F. *et al.* Progression of Parkinson's disease pathology is reproduced by intragastric administration of rotenone in mice. *PLoS One* **5**, e8762 (2010).
9. Li, J. Y. *et al.* Lewy bodies in grafted neurons in subjects with Parkinson's disease suggest host-to-graft disease propagation. *Nat Med* **14**, 501–503 (2008).
10. Kordower, J. H., Chu, Y., Hauser, R. A., Freeman, T. B. & Olanow, C. W. Lewy body-like pathology in long-term embryonic nigral transplants in Parkinson's disease. *Nat Med* **14**, 504–506 (2008).
11. Brundin, P., Li, J. Y., Holton, J. L., Lindvall, O. & Revesz, T. Research in motion: the enigma of Parkinson's disease pathology spread. *Nat Rev Neurosci* **9**, 741–745 (2008).
12. Desplats, P. *et al.* Inclusion formation and neuronal cell death through neuron-to-neuron transmission of alpha-synuclein. *Proc Natl Acad Sci U S A* **106**, 13010–13015 (2009).
13. Alvarez-Erviti, L. *et al.* Lysosomal dysfunction increases exosome-mediated alpha-synuclein release and transmission. *Neurobiol Dis* **42**, 360–367 (2011).
14. Lorincz, M. T. Clinical implications of Parkinson's disease genetics. *Semin Neurol* **26**, 492–498 (2006).
15. Amaravadi, R. K. *et al.* Principles and current strategies for targeting autophagy for cancer treatment. *Clin Cancer Res* **17**, 654–666.
16. Lebovitz, C. B., Bortnik, S. B. & Gorski, S. M. Here, there be dragons: charting autophagy-related alterations in human tumors. *Clin Cancer Res* **18**, 1214–1226.
17. Checkoway, H. & Nelson, L. M. Epidemiologic approaches to the study of Parkinson's disease etiology. *Epidemiology* **10**, 327–336 (1999).
18. Gorell, J. M., Johnson, C. C., Rybicki, B. A., Peterson, E. L. & Richardson, R. J. The risk of Parkinson's disease with exposure to pesticides, farming, well water, and rural living. *Neurology* **50**, 1346–1350 (1998).
19. Tanner, C. M. *et al.* Rotenone, paraquat, and Parkinson's disease. *Environ Health Perspect* **119**, 866–872 (2011).
20. Monville, C., Torres, E. M. & Dunnett, S. B. Comparison of incremental and accelerating protocols of the rotarod test for the assessment of motor deficits in the 6-OHDA model. *J Neurosci Methods* **158**, 219–223 (2006).
21. Greene, J. G., Noorian, A. R. & Srinivasan, S. Delayed gastric emptying and enteric nervous system dysfunction in the rotenone model of Parkinson's disease. *Exp Neurol* (2009).
22. Edwards, L. L., Quigley, E. M. & Pfeiffer, R. F. Gastrointestinal dysfunction in Parkinson's disease: frequency and pathophysiology. *Neurology* **42**, 726–732 (1992).
23. Ling, E. A., Shieh, J. Y., Wen, C. Y., Yick, T. Y. & Wong, W. C. The dorsal motor nucleus of the vagus nerve of the hamster: ultrastructure of vagal neurons and their responses to vagotomy. *J Anat* **152**, 161–172 (1987).
24. Braak, H., Rub, U., Gai, W. P. & Del Tredici, K. Idiopathic Parkinson's disease: possible routes by which vulnerable neuronal types may be subject to neuroinvasion by an unknown pathogen. *J Neural Transm* **110**, 517–536 (2003).
25. Prasad, K. & Richfield, E. K. Number and nuclear morphology of TH+ and TH- neurons in the mouse ventral midbrain using epifluorescence stereology. *Exp Neurol* **225**, 328–340 (2010).
26. Ltic, S. *et al.* Alpha-synuclein is expressed in different tissues during human fetal development. *J Mol Neurosci* **22**, 199–204 (2004).
27. Hasegawa, T. *et al.* The AAA-ATPase VPS4 regulates extracellular secretion and lysosomal targeting of alpha-synuclein. *PLoS One* **6**, e29460.
28. Campenot, R. B. Development of sympathetic neurons in compartmentalized cultures. II. Local control of neurite growth by nerve growth factor. *Dev Biol* **93**, 1–12 (1982).
29. Campenot, R. B. Independent control of the local environment of somas and neurites. *Methods Enzymol* **58**, 302–307 (1979).
30. Pautot, S., Wyart, C. & Isacoff, E. Y. Colloid-guided assembly of oriented 3D neuronal networks. *Nat Methods* **5**, 735–740 (2008).
31. Vernier, P. *et al.* The degeneration of dopamine neurons in Parkinson's disease: insights from embryology and evolution of the mesostriatocortical system. *Ann N Y Acad Sci* **1035**, 231–249 (2004).
32. Betarbet, R. *et al.* Chronic systemic pesticide exposure reproduces features of Parkinson's disease. *Nat Neurosci* **3**, 1301–1306 (2000).
33. Greenamyre, J. T., Betarbet, R. & Sherer, T. B. The rotenone model of Parkinson's disease: genes, environment and mitochondria. *Parkinsonism Relat Disord* **9** Suppl 2, S59–64 (2003).
34. Miwa, H., Kubo, T., Suzuki, A., Nishi, K. & Kondo, T. Retrograde dopaminergic neuron degeneration following intrastriatal proteasome inhibition. *Neurosci Lett* **380**, 93–98 (2005).



35. Klein, R. M. & McKenzie, J. C. Pattern of crypt cell proliferation in the pre- and post-closure ileum of the neonatal rat: effects of sympathectomy. *Cell Tissue Res* **206**, 387–394 (1980).
36. Holle, G. E., Granat, T., Reiser, S. B. & Holle, F. Effects of superior mesenteric and coeliac ganglionectomy on the small intestinal mucosa in the Hanford mini pig. I. Histological and enzyme-histochemical study. *J Auton Nerv Syst* **26**, 135–145 (1989).
37. Santos, J. *et al.* Corticotropin-releasing hormone mimics stress-induced colonic epithelial pathophysiology in the rat. *Am J Physiol* **277**, G391–399 (1999).
38. Bhatia, V. & Tandon, R. K. Stress and the gastrointestinal tract. *J Gastroenterol Hepatol* **20**, 332–339 (2005).
39. Francardo, V. *et al.* Impact of the lesion procedure on the profiles of motor impairment and molecular responsiveness to L-DOPA in the 6-hydroxydopamine mouse model of Parkinson's disease. *Neurobiol Dis* **42**, 327–340 (2011).
40. Danzer, K. M. *et al.* Exosomal cell-to-cell transmission of alpha synuclein oligomers. *Mol Neurodegener* **7**, 42 (2012).
41. Danzer, K. M. *et al.* Different species of alpha-synuclein oligomers induce calcium influx and seeding. *The Journal of neuroscience : the official journal of the Society for Neuroscience* **27**, 9220–9232 (2007).
42. Elkon, H. *et al.* Mutant and wild-type alpha-synuclein interact with mitochondrial cytochrome C oxidase. *J Mol Neurosci* **18**, 229–238 (2002).
43. Esteves, A. R., Arduino, D. M., Silva, D. F., Oliveira, C. R. & Cardoso, S. M. Mitochondrial Dysfunction: The Road to Alpha-Synuclein Oligomerization in PD. *Parkinsons Dis* **2011**, 693761 (2011).
44. Schmidt, F. *et al.* Single-channel electrophysiology reveals a distinct and uniform pore complex formed by alpha-synuclein oligomers in lipid membranes. *PLoS One* **7**, e42545 (2012).
45. Choi, W. S., Palmiter, R. D. & Xia, Z. Loss of mitochondrial complex I activity potentiates dopamine neuron death induced by microtubule dysfunction in a Parkinson's disease model. *J Cell Biol* **192**, 873–882 (2011).
46. Rajendran, L. *et al.* Alzheimer's disease beta-amyloid peptides are released in association with exosomes. *Proc Natl Acad Sci U S A* **103**, 11172–11177 (2006).

Acknowledgements

We would like to thank Marino Zerial (MPI-CBG, Dresden, Germany) for laboratory space, reagents and the helper plasmids to generate the virus and culture transfected cells. Brian Spencer (California University, La Jolla, USA) for the plasmid containing the alpha-synuclein gene. K-H Schäfer Laboratory (Zweibrücken, Germany) for showing us their ENS isolation protocol. Prof. Lawrence Rajendran (ETH, Zurich, Switzerland) for sharing and helping with the exosome isolation protocol. Prof. Solimena for letting us use their Bioimager and Prof. Kempermann for letting us use the rotarod equipment (both from TU-Dresden, Dresden, Germany). We would also like to thank Prof. Alexander Storch (TU-Dresden, Dresden, Germany) for stimulating scientific discussions. This work was supported by the Fritz-Thyssen Foundation, the German Parkinson's disease Society and by Amelia Jimenez Gomez as private donor.

Authors contributions

F.P.-M. designed all experiments in the study. F.P.-M. and M.S. performed the in vivo experiments. F.P.-M. and M.S. performed the in vivo work and made the stereological and image quantification analysis. F.P.-M., M.A. and C.W. performed the cell culture, exosome isolation and western-blot for the in vitro single cell cultures. F.P.-M. and C.W. developed and performed the Campenot chamber experiments for the in vitro co-culture experiments. F.P.-M. and A.P. designed and cloned the mCherry-alpha-synuclein plasmid for the lentivirus. G.A.O. performed the live video microscopy. G.M. performed the statistical analysis on the EM data. F.P.-M. coordinated the project and wrote the manuscript with the help of G.M., G.O., M.R.-A., G.G., R.H.W.F. and H.R.

Additional information

Supplementary information accompanies this paper at <http://www.nature.com/scientificreports>

Competing financial interests: The authors declare no competing financial interests.

License: This work is licensed under a Creative Commons Attribution-NonCommercial-NoDerivs 3.0 Unported License. To view a copy of this license, visit <http://creativecommons.org/licenses/by-nc-nd/3.0/>

How to cite this article: Pan-Montojo, F. *et al.* Environmental toxins trigger PD-like progression via increased alpha-synuclein release from enteric neurons in mice. *Sci. Rep.* **2**, 898; DOI:10.1038/srep00898 (2012).